The Oxidation Reaction in X-Irradiated Bis(ethylenediamine)platinum(II) Bis(hydrogen squarate): A Single-Crystal EPR Study of a Platinum(III) Complex

Michel Geoffroy,*[1a] Gérald Bernardinelli,[1a] Paule Castan,*[1b] Henry Chermette,*[1a,c] Diane Deguenon,[1b] Safouh Nour,[1c] Jacques Weber,[1a] and Michel Wermeille[1a]

Departement de Chimie Physique et Laboratoire de Cristallographie, 30 quai E. Ansermet, Université de Genève, 1211 Genève, Switzerland, Laboratoire de Chimie Inorganique, 205 route de Narbonne, Université Paul Sabatier, 31077 Toulouse, France, and Institut de Physique Nucléaire de Lyon, Université Claude Bernard, 69622 Villeurbanne, France

Received November 19, 1991

A large single crystal of bis(ethylenediamine)platinum bis(hydrogen squarate) ($[Pt(en)_2](HSq)_2$), has been X-irradiated at 77 K and studied by EPR. The **g** and ^{195}Pt hyperfine tensors obtained from the angular dependence of the spectrum are consistent with the trapping of a Pt(III) complex containing the unpaired electron in a d_{z^2} orbital. Comparison of the orientations of the eigenvectors with those of the crystallographic interatomic vectors together with the predictions of Xα calculations on the model complex $[Pt(NH_3)_4(OH)_2]^+$ leads to a mechanism whereby a radiogenic radical, formed by homolytic scission of the hydrogen squarate hydroxyl, oxidizes the $Pt(en)_2$ dication and yields $[Pt(en)_2(Sq)](HSq)$.

Introduction

Over the past few years there has been much interest in the chemistry of complexes in which a metal ion presents an unusual oxidation state.[2-5] Some of these compounds are expected to exhibit interesting physicochemical properties, and for example, several studies have been devoted to the electrical conductivity of platinum mixed-valence complexes and of Pt(III) complexes.[6-8] However, experimental information on the electronic structure of these complexes is difficult to obtain since, a few cases excepted,[9] these compounds are unstable or amorphous. When good crystals are obtained, the compound is a di- or a polymetallic species with metal–metal bonds and does not present magnetic properties.[10] The most appropriate technique for the study of a monomeric Pt(III) complex is certainly to trap this paramagnetic species in a diamagnetic single-crystal matrix and to perform an EPR study.[6,11,12] Such complete studies yielding the **g** and ^{195}Pt hyperfine tensors for an organic complex of Pt(III) remain nevertheless rare. Moreover, in most studies the Pt(III) species have been produced by photolysis or radiolysis of Pt(II) or Pt(IV) precursors[12-15] which contain one or several halogen atoms; the reactivity of these halogens then yields a large variety of secondary reactions that make the identification of the paramagnetic species difficult.

In the present study, we have selected a Pt(II) precursor, $[Pt(en)_2](HSq)_2$, which presents the following properties: (1) it is expected to give few secondary reactions; no halogen atom is present in the compound and electroneutrality is ensured by large oxocarbon anions which could migrate only with difficulty in the crystal matrix; (2) its crystal system, triclinic, facilitates the EPR analysis since all the complexes of the same species are magnetically equivalent for each orientation of the magnetic field; (3) its crystal structure is known[16] and enables us to determine the orientation of the various EPR eigenvectors (**g** and ^{195}Pt hyperfine coupling) with respect to the bond directions of the Pt(II) precursor. Such an analysis, together with the predictions of multiple scattering (MS) molecular orbital (MO) Xα calculations on the model compound $[Pt(NH_3)_4(OH)_2]^+$, not only gives information on the structure of the Pt(III) complex but also suggests a mechanism for the oxidation of the Pt(II) precursor.

Experimental Section

MS Xα Calculations. In order to facilitate the MS Xα investigations, the $Pt(en)_2$ ion was replaced, in the calculations, by $[Pt(NH_3)_4]$, for which a C_{4v} symmetry has been assumed. The nitrogen atoms are located on the bisectors of the x and y axes. We started our calculations by locating a squarate ligand on both sides of the PtN_4 plane with an interplane distance of 3.6 Å. Under these conditions, the MS Xα scheme leads to a poor modeling of the complex because of the muffin-tin approximation used in this method: one is led to calculate a bulky molecule with a large outer-sphere radius and—more dramatically—a large intersphere region (where the potential is assumed to be constant) which plays a major role in the description of the electronic structure. We have therefore tried to model the complex by using smaller diamagnetic ligands in the axial positions. The OH^- ion has been chosen for the following reasons: (i) it has the same charge as the squarate ion, (ii) it is diamagnetic, and (iii) it can preserve the C_{4v} symmetry of the complex. This approach leads to a more compact complex, with a much smaller role played by the intersphere in the description of the potential.

(1) (a) Université of Genève. (b) Université Paul Sabatier. (c) Université Claude Bernard.
(2) Geiger, W. E.; Allen, C. S.; Mines, T. E.; Senftleber, F. C. *Inorg. Chem.* **1977**, *16*, 2003.
(3) Wyatt, J. L.; Symons, M. C. R.; Hasegawa, A. *J. Chem. Soc., Faraday Trans. 1* **1987**, *83*, 2803.
(4) Arrizabalaga, P.; Bernardinelli, G.; Geoffroy, M.; Castan, P.; Dahan, F. *Chem. Phys. Lett.* **1986**, *124*, 549.
(5) Kirmse, R.; Stach, J.; Dietzsch, W.; Steinmecke, G.; Hoyer, E. *Inorg. Chem.* **1980**, *19*, 2679.
(6) Kawamori, A.; Aoki, R.; Yamashita, M. *J. Phys. C, Solid State Phys.* **1985**, *18*, 5487.
(7) Hamane, Y.; Ashi, R.; Yamahita, M.; Kida, S. *Inorg. Chim. Acta* **1981**, *54*, L13.
(8) Interrante, L. V.; Browall, K. W. *Inorg. Chem.* **1974**, *13*, 1162.
(9) Uson, R.; Forniés, J.; Tomas, M.; Menjon, B.; Bau, R.; Sunkel, K.; Kuwabara, E. *Organometallics* **1986**, *5*, 1576.
(10) Hollis, L. S.; Roberts, M. M.; Lippard, S. J. *Inorg. Chem.* **1983**, *22*, 3637 and references therein. Che, C. M.; Mak, T. C. W.; Miskowski, V. M.; Gray, H. B. *J. Am. Chem. Soc.* **1986**, *108*, 7840. Che, C. M.; Herbstein, F. M.; Schaefer, W. P.; Marsh, R. E.; Gray, H. B. *J. Am. Chem. Soc.* **1983**, *105*, 4604. Che, C. M.; Shaefer, W. P.; Gray, H. B.; Dickson, M. K.; Stein, P. B.; Roundhill, D. M. *J. Am. Chem. Soc.* **1982**, *104*, 4253.
(11) Kirmse, R.; Dietzsch, W.; Solov'ev, B. V. *J. Inorg. Nucl. Chem.* **1977**, *39*, 1157.
(12) Krigas, T.; Rogers, M. T. *J. Chem. Phys.* **1971**, *55*, 3035.
(13) Nizova, G. V.; Serdobov, M. V.; Nikitaev, A. T.; Shul'pin, G. B. *J. Organomet. Chem.* **1984**, *275*, 139.
(14) Shagisultanova, G. A.; Karaban, A. A. *Russ. J. Phys. Chem.* (*Engl. Transl.*) **1971**, *45*, 1652.
(15) Shubochkin, L. K.; Gishchin, V. I.; Larin, G. M.; Koloso, V. A. *Russ. J. Inorg. Chem. Engl. Transl.* **1974**, *19*, 249.
(16) Castan, P.; Deguenon, D.; Fabre, P. L.; Bernardinelli, G. *Polyhedron* **1992**, *8*, 901.

0020-1669/92/1331-5056$03.00/0

Table I. Upper Valence Ground-State Energy Levels and Charge Distribution of $[Pt(NH_3)_4]^{3+}$, $[Pt(NH_3)_4(OH)_2]^{+}$, and $\{[Pt(NH_3)_4(OH)](OH)\}^{+}$ As Calculated by the MS X_α Method

			$[Pt(NH_3)_4]^{3+}$ [a]			$[Pt(NH_3)_4(OH)_2]^{+}$ [b]				$\{[Pt(NH_3)_4(OH)](OH)\}^{+}$ [c]			$\{[Pt(NH_3)_4(OH)](OH)\}^{+}$ [d]		
label	occ	d orbital	energy (eV)	% d	% s	label	occ	energy (eV)	% d	% s	energy (eV)	% d	% s	energy (eV)	% d	% s
$4b_2\downarrow$	0	d_{xy}	−18.0	54		$4b_2\downarrow$	0	−6.8	60		−9.6	58		−9.7	57	
$4b_2\uparrow$	0	d_{xy}	−18.3	52		$4b_2\uparrow$	0	−7.1	59		−9.9	56		−9.9	56	
$4a_1\downarrow$	1	d_{z^2}	−24.4	63	20	$9a_1\downarrow$	0	−8.5	61	3	−13.1	52	7	−13.2	49	7
$4a_1\uparrow$	1	d_{z^2}	−24.9	60	22	$9a_1\uparrow$	1	−9.0	60	3	−13.5	51	7	−13.6	48	8
$2b_1\downarrow$	0	$d_{x^2-y^2}$	−24.1	88		$2b_1\downarrow$	1	−12.5	89		−15.6	88		−15.6	89	
$5e\downarrow$	2	d_{xz}, d_{yz}	−24.4	88		$6e\downarrow$	2	−13.3	65		−16.3	75		−16.0	78	
$2b_1\uparrow$	1	$d_{x^2-y^2}$	−24.7	86		$2b_1\uparrow$	1	−12.9	89		−16.0	88		−16.0	88	
$5e\uparrow$	2	d_{xz}, d_{yz}	−25.0	87		$6e\uparrow$	2	−13.7	68		−16.7	76		−16.4	80	
$3a_1\downarrow$	1	d_{z^2}	−27.9	23	21	$7a_1\downarrow$	1	−17.6	27	15	−20.3	17	25	−20.2	36	1
$3a_1\uparrow$	1	d_{z^2}	−28.1	27	20	$6a_1\downarrow$	1	−18.1	13	17	−21.6			−20.3		30
$3b_2\downarrow$	1	d_{xy}	−28.2	54		$7a_1\uparrow$	1	−17.7	22	19	−20.5	17	25	−20.4	25	18
$3b_2\uparrow$	1	d_{xy}	−28.5	55		$3b_2\downarrow$	1	−17.6	48		−20.5	51		−20.4	50	
						$6a_1\uparrow$	1	−18.4	18	13	−21.6			−20.6	12	13
						$3b_2\uparrow$	1	−17.8	50		−20.7	53		−20.6	50	
						$5a_1\downarrow$	1				−22.2	5	15			
						$5a_1\uparrow$	1				−22.5	5	15			

[a] Pt–N distance = 3.85 au. [b] Pt–O distance = 4.02 au. [c] Pt–O1 distance = 3.82 au, Pt–O2 distance = 5.72 au. [d] Pt–O1 distance = 4.02 au, Pt–O2 distance = 5.52 au, N–Pt distance = 3.86 au (Pt atom above the N_4 plane by 0.2 au).

In the classical muffin-tin description, each atom is surrounded by a sphere in which the electronic potential is spherically averaged. The nonempirical procedure of Norman[17] is used to obtain the overlapping-sphere radii (Pt, 2.91 au; N, 1.50 au; H, 0.96 au; O, 1.75 au), and the values of α are taken from the compilation of Schwarz.[18] A weighted average of the atomic values of α is chosen for the interatomic and extramolecular regions. Partial waves up to $l = 3$ are included in the multiple-scattering expansions in the Pt sphere, up to $l = 4$ for the extramolecular region and up to $l = 1$ for N, O, and H spheres.

All these calculations have been performed without any charged Watson sphere in order to have the same effect of the environment for clusters with different ionicity. Relativistic effects are taken into account by addition of the mass-velocity and Darwin terms in the last loops of the self-consistent field (SCF) procedure. Once self-consistency is reached, a SCF spin-polarized calculation is performed in order to show the dependence of the energy levels on the spin polarization.

In the spin-polarized (SP) MS Xα formalism, the Fermi contact interaction is given[19] by

$$A_F = 8\pi g_e\beta_e g_n\beta_n[\rho^{\uparrow}(0) - \rho^{\downarrow}(0)]/3$$

where $\rho^{\uparrow}(0)$ and $\rho^{\downarrow}(0)$ are the spin-up and spin-down electronic densities at the nucleus.

The contribution to the dipolar hyperfine coupling of the d orbital which participates in the MO Ψ_k is obtained from

$$\tau = g_e\beta_e g_n\beta_n\alpha_i[n^{\uparrow}_k\rho^{\uparrow}_k\langle r^{-3}\rangle^{\uparrow}_k - n^{\downarrow}_k\rho^{\downarrow}_k\langle r^{-3}\rangle^{\downarrow}_k]$$

where α_i is a proper angular factor, n_k is the occupation number of the MO $\Psi^{\uparrow\downarrow}_k$, $\rho^{\uparrow\downarrow}_k$ is the gross d metal population of this orbital, and $\langle r^{-3}\rangle_k$ is the radical expectation value calculated for this MO.

Compound Preparation, Irradiation, and EPR Analysis. $[Pt(en)_2](HSq)_2$ was synthesized[16] by addition of a solution of squaric acid to an aqueous solution of $[Pt(en)_2]Cl_2$. A single crystal of $[Pt(en)_2](HSq)_2$, obtained by slow evaporation of an aqueous solution, was glued onto a small brass cube and irradiated during 3.5 h, at 77 K, using a Philips X-ray tube equipped with a tungsten anticathode. Immediately after irradiation, the crystal was transferred, without any warming, in a finger dewar inserted in the cavity of a Bruker E-200 ESR spectrometer (X-band, 100-kHz field modulation). The EPR tensors were obtained by recording the angular dependence of the signals in three perpendicular planes (steps of 10°). The mutual orientation of the crystallographic and EPR reference axes was determined from diffractometer measurements on the EPR sample. The matrix which transforms the fractional coordinates (abc system) into the Cartesian coordinates (*XYZ*) is given in ref 20. The EPR analysis was performed by using a Hamiltonian which takes into account the electronic and nuclear Zeeman effects as well as the hyperfine interaction with ^{195}Pt (^{195}Pt: natural abundance = 33.8%, $I = 1/2$). The elements of the EPR tensors were determined by minimizing[21] the function $F = \Sigma_{i,j}|H_{ij}(\text{exp}) - H_{ij}(\text{calc})|$ where i and j characterize the orientation of the magnetic field and the EPR transition, respectively. The field positions H_{ij}(calc) were obtained from a second-order perturbation calculation. The **g** tensor was first determined by only taking the signals due to the nonmagnetic Pt isotope into account; then the resulting tensor was fixed, and the ^{195}Pt hyperfine tensor was obtained from the satellite signals.

Results

MS Xα Calculations. As expected, when relativistic corrections are included in the calculations, the Pt s and p levels are stabilized, in contrast with the d and f orbitals.[22] The energy levels of the various molecular orbitals calculated for $[Pt(NH_3)_4]^{3+}$ are shown in Table I together with those corresponding to $[Pt(NH_3)_4(OH)_2]^{+}$. For this last complex two cases have been considered: (1) each OH group is located at the same distance from the metal atom; (2) one Pt–O distance is shortened whereas the other one is elongated. In the platinum(III) compound[23] $Na_2[Pt_2(HPO_4)_4(H_2O)_2]$, a water molecule is coordinated at each axial position of the $Pt_2(HPO_4)_4$ unit and the Pt–O(H_2O) bond length is equal to 2.15 Å, while in the platinum(II) complex[24] $[Pt(NH_3)_2C_4O_4]_4$ the squaric moiety is coordinated to platinum and exhibits a mean Pt–O(squaric) distance of 2.02 Å. The Pt–O(OH) distances used for the MS Xα calculations on $[Pt(NH_3)_4(OH)_2]^{+}$ have therefore been chosen to be ca. 2 Å and are mentioned in Table I together with the contributions of the 5d and 6s orbitals.

The MS Xα results shown in Table I indicate that for the $[Pt(NH_3)_4]^{3+}$ compound the d_{z^2} orbital ($4a_1$) lies below both the d_{xy} ($4b_2$, antibonding d_{xy}–N_{2p} MO) and $d_{x^2-y^2}$ ($2b_1$) orbitals. Therefore, for this Pt(III) species, the SOMO has a predominant $d_{x^2-y^2}$ character. This order of the energy levels is however modified when one or two hydroxyl ions are added on the *z* axis at a distance sufficiently close to the platinum atom. In this case, an upward shift of the d_{z^2} orbital energy relative to those of the other d orbitals (mainly $d_{x^2-y^2}$) is observed. Such an effect is, of course, related to the σ bonding/antibonding interaction between

(17) Norman, J. G., Jr. *J. Chem. Phys.* **1974**, *61*, 4630.
(18) Schwarz, K. *Phys. Rev.* **1974**, *B5*, 2466; *Theor. Chim. Acta* **1974**, *34*, 225.
(19) Weber, J. In *Current Aspects of Quantum Chemistry*; Carbo, R., Ed.; Elsevier: Amsterdam, 1982; p 437.
(20) The three columns of the matrix which transforms the fractional crystallographic coordinates into the Cartesian coordinates expressed in the ESR reference frame are respectively (−4.0270, 5.5759, 0.5492), (−6.4339, −4.7117, 0.8319), and (−3.8370, 0.1294, 7.5429).
(21) James, F.; Roos, M. *CERN Program Library*; CERN: Geneva, Switzerland, 1976.
(22) Pykko, P. *Chem. Rev.* **1988**, *88*, 563.
(23) Cotton, F. A.; Falvello, L. R.; Scott, H. *Inorg. Chem.* **1982**, *21*, 1709.
(24) Bernardinelli, C.; Castan, P.; Soules, R. *Inorg. Chim. Acta* **1986**, *120*, 205.

Table II. Hyperfine Interaction (MHz) As Calculated by the MS Xα Method (Spin Polarized) for $[Pt(NH_3)_4(OH)_2]^+$ and $\{[Pt(NH_3)_4(OH)](OH)\}^+$

complex	I[a]	II[b]	III[c]
Fermi contact			
total	250	925	953
Pt 6s contribn	462	1072	1142
Dipolar coupling			
d_{z^2} contribn[d]	681	540	508

[a] Pt–O distance = 4.02 au. [b] Pt–O1 distance = 3.82 au, Pt–O2 distance = 5.72 au. [c] Pt–O1 distance = 4.02 au, Pt–O2 distance = 5.52 au, N–Pt distance = 3.86 au (Pt atom above the N_4 plane by 0.2 au). [d] Anisotropic coupling along the normal to the plane containing the four nitrogen atoms.

the oxygen 2p-σ orbital and the $5d_{z^2}$ orbital, which increases when the Pt–O distance decreases. In fact, this is a three-level system because the Pt 6s orbital is strongly involved in this process. The various electronic populations of the xa_1 orbitals ($x = 6, 7, 9$) are given in Table I. This trend is similar to that previously noticed by Goursot et al.[25,26] for $PtCl_4$ and $PtCl_6$ complexes; but the important point is that it is not necessary that *both* of the two hydroxyl ligands be sufficiently close to the platinum atom for locating the unpaired electron in the $9a_1$ orbital. Indeed, if a single OH^- ion lies far from the Pt(III) atom, its MO's do not mix significantly with the MO's of the complex, and in fact, they just lie above some of the d orbitals; in that case, which in fact corresponds to $\{[Pt(NH_3)_4(OH)]^{2+},(OH)^-\}$, one has not to fulfill the Fermi statistics during the calculation, keeping the $9a_1$ MO containing the d_{z^2} orbital filled with a single electron. This is the true SOMO as it appears when the two ligands are sufficiently close to the Pt atom, but then, this is also the case of a single OH group kept bonded to $Pt(NH_3)_4$. It is worthwhile noticing that no dramatic change in the energy diagram can be observed if the decrease of the Pt–OH bond length is not obtained by moving the OH ligand toward the PtN_4 plane but is reached by moving the Pt atom out of the N_4 plane toward one OH group. Therefore the main result is the presence of a strong d_{z^2} character in the SOMO of the Pt(III) complex, provided that at least one Pt–OH bond length is short enough. In the meantime, it is important to note that the SOMO exhibits a significant Pt 6s character which is responsible for the spin density at the Pt nucleus (spin-polarized calculation), which is directly related to the isotropic Fermi contact term of the hyperfine tensor.

For $[Pt(NH_3)_4(OH_2)]^+$ and $\{[Pt(NH_3)_4(OH)]^{2+},(OH)^-\}$, the ^{195}Pt dipolar hyperfine coupling is expected to arise essentially from the participation of the d_{z^2} orbital in the $9a_1$ MO. This contribution together with the Fermi interaction has been obtained from the NSP MS Xα calculations for the selected structures shown in Table I. These values are given in Table II together with the contribution of the 6s orbital to the Fermi interaction.

Electron Paramagnetic Resonance. An example of an EPR spectrum recorded at 77 K with a single crystal of $[Pt(en)_2](HSq)_2$ immediately after X-irradiation at 77 K is shown in Figure 1. Three groups of lines are observed on this spectrum: a very intense signal marked C, an anisotropic intense signal B, and a weak signal A on each side of B. The central signal C is rather isotropic and suggests the trapping of an organic radical. The temperature dependence of the spectrum shows that both the contributions A and B suddenly disappear when the temperature reaches 200 K. The angular variation of signals A and B is shown in Figure 2. These curves indicate that signals A are in fact satellite lines of signal B and their intensity indicates that they can be attributed to the isotope ^{195}Pt. For some orientations of the crystal, the high-field transition A or signal B is hidden by the intense signal C; nevertheless, the g and ^{195}Pt hyperfine tensors can be obtained without any ambiguity, since at least two of the three lines are observed for almost all the orientations. These tensors are given in Table III. In accord with the crystal structure (triclinic, $P\bar{1}$) only one orientation of the paramagnetic species is detected for each orientation of the sample.

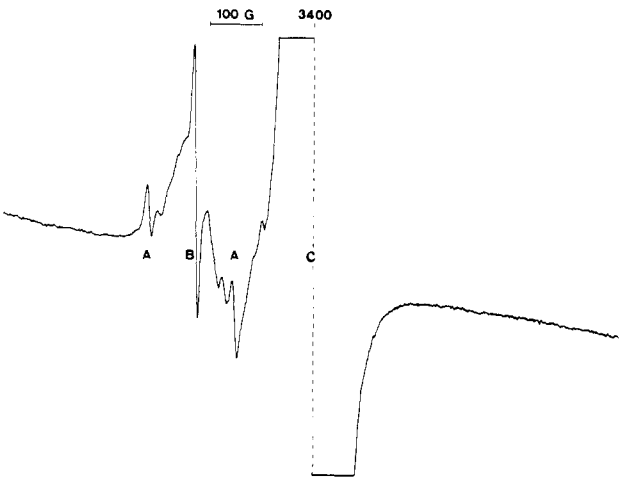

Figure 1. Example of an EPR spectrum obtained at 77 K with a single crystal of $[Pt(en)_2](HSq)_2$ after X-irradiation at 77 K.

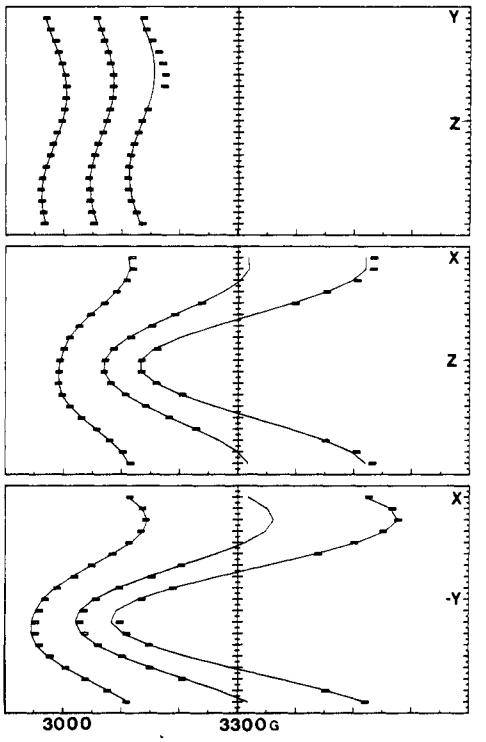

Figure 2. Angular variation of the EPR signals obtained with an X-irradiated single crystal of $[Pt(en)_2](HSq)_2$.

Discussion

The crystal structure of $[Pt(en)_2](HSq)_2$ consists of separate $[(Pt(en)_2]^{2+}$ and HSq^- entities forming alternating layers[16] as shown in Figure 3. In the cation, the platinum atom is coordinated in a square geometry to four nitrogen atoms (Pt–N = 2.03 Å, N1PtN2 = 84.4°, N2PtN1′ = 95°). The nonequivalence of the oxygen atoms in the hydrogen squarate monoanion is clearly seen from the carbon–oxygen bond lengths: for O3 and O4 this distance is equal to 1.23 Å (double bond), for O2 its participation in a hydrogen bond with the hydroxyl of a second hydrogen squarate monoanion causes a slight increase of this bond length (1.26 Å), and for O1—the hydroxyl oxygen—this bond length is equal to 1.32 Å. The squarate ions therefore form planar dimers,

(25) Goursot, A.; Chermette, H. *Can. J. Chem.* **1987**, *63*, 1407.
(26) Goursot, A.; Chermette, H.; Chanon, M.; Waltz, W. L. *Inorg. Chem.* **1985**, *24*, 1042. Goursot, A.; Chermette, H.; Penigault, E.; Chanon, M.; Waltz, W. L. *Inorg. Chem.* **1984**, *23*, 3618.

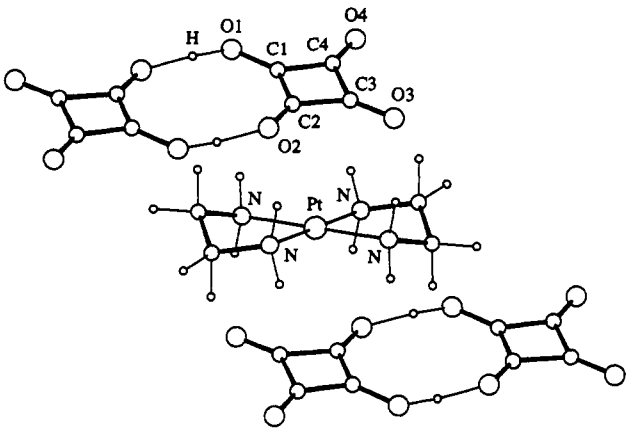

Figure 3. Mutual orientation of the hydrogen squarate and bis(ethylenediamine)platinum ions in a crystal of [Pt(en)$_2$](HSq)$_2$.

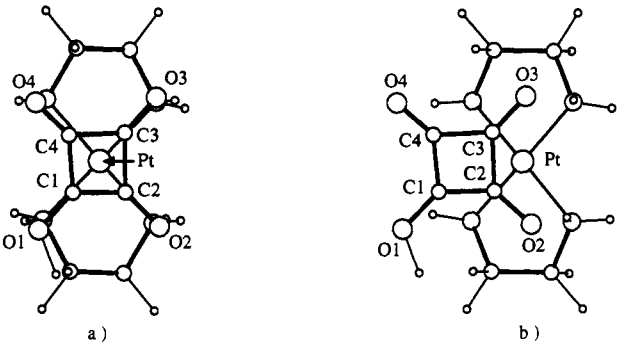

Figure 4. Projection of the atoms of the $[Pt(en)_2]^{2+}$ and $(HSq)^-$ ions in (a) the PtN_4 plane and (b) the hydrogen squarate plane.

Table III. Experimental g and ^{195}Pt Hyperfine Tensors Obtained with an X-Irradiated Single Crystal of [Pt(en)$_2$](HSq)$_2$[a]

	eigenvectors		
eigenvalues	*X*	*Y*	*Z*
g tensor			
$g_1 = 1.971$	−0.9360	−0.3342	−0.1096
$g_2 = 2.162$	−0.1684	0.1524	0.9738
$g_3 = 2.198$	0.3088	−0.9300	0.1990
^{195}Pt *T* (MHz)			
$T_1 = 1197$	−0.9601	−0.2741	−0.0543
$T_2 = 410$	0.0452	−0.3444	0.9377
$T_3 = 412$	0.2757	−0.8979	−0.3431

[a] Estimated errors are as follows. On eigenvalues: g_1, ±0.001; g_2 and g_3, ±0.003; T_1, ±10 MHz; T_2 and T_3, ±30 MHz. On the orientation of eigenvectors: g_1, ±3°; T_1, ±4°.

and the corresponding molecular plane makes an angle of 20° with the PtN_4 plane. The vector connecting the Pt atom to the squarate center is oriented perpendicular to the PtN_4 plane (Figure 4a), and the corresponding distance is equal to 3.3 Å.

Exposure of a Pt(II) complex to ionizing radiation is expected to yield either the Pt(I) or the Pt(III) complex. It is known from ligand field theory[27] that a planar complex with $5d^9$ configuration is characterized by $g_\parallel > g_\perp > g_e$ and $T_{\parallel(\text{metal})} \parallel g_\parallel$ whereas a $5d^7$ complex with elongated D_{4h} structure is characterized by $g_\parallel < g_\perp$ and $T_{\parallel(\text{metal})} \parallel g_\parallel$. The g tensor obtained for the radiogenic complex (Table II) is strongly anisotropic and exhibits axial symmetry ($|g_1 - g_2| = 0.191$, $|g_2 - g_3| = 0.036$) with $g_\parallel = 1.971$ and $g_{\perp_{av}} = 2.180$. The ^{195}Pt hyperfine tensor (Table III) exhibits a strong axial symmetry and the ^{195}Pt–$T_\parallel$ direction is almost aligned along the g_{min} direction (g_{min}, $T_\parallel = 5°$).

These properties are consistent with a d^7 ion (low-spin configuration) containing the unpaired electron in a d_{z^2} orbital, and signals A and B will therefore be assigned to a Pt(III) species formed by oxidation of $[Pt(en)_2]^{2+}$. As shown below, the Xα calculations are indeed consistent with a d_{z^2} ground state, and we will use expressions of g and hyperfine couplings derived from those previously given by Maki[28] and by McGarvey.[29] In the axial approximation

$$g_\parallel = 2.0023 - 3c_1^2$$

$$g_\perp = 2.0023 + 6c_1 - 6c_1^2$$

$$T_\parallel = K + P(4/7 - 6c_1/7 + 15c_1^2/7)$$

$$T_\perp = K + P(-2/7 + 45c_1/7 - 57c_1^2/14)$$

where c_1 represents the mixing of the ^{2}E excited state into the ground state by spin–orbit coupling ($c_1 = \xi/\Delta(^2E)$; additional c_i terms due to the contribution of other excited states are assumed to be negligible). *K* represents the Fermi contact parameter, *P* is the equal to $g_e\beta_e g_n\beta_n\langle r^{-3}\rangle$. The values of *K* and *P* can be estimated from the hyperfine eigenvalues by using, for c_1, the average value ($c_1 = 0.065 \pm 0.035$) found from $g_\parallel$ and $g_\perp$. The signs of the experimental hyperfine eigenvalues are unfortunately unknown, but the single combination which leads to a value of *P* (1830 MHz) similar to the atomic constant given by Morton and Preston ($P_0 = 1470$ MHz)[30] corresponds to $T_\parallel$ and $T_\perp$ both positive. The resulting value of *K* (+226 MHz)[31] indicates that the Fermi contact interaction is not only due to internal spin polarization and that some metal 6s orbital probably participates in the SOMO.

As shown in Table I, the MS Xα results agree with a strong participation of the metal d_{z^2} orbital in the SOMO only if one or two ligands are located sufficiently close to the platinum atom. For the two pentacoordinated structures (Table II), the component of the dipolar ^{195}Pt hyperfine interaction, aligned perpendicular to the plane containing the four nitrogen atoms, is in excellent accordance with the experimental anisotropic coupling (524 MHz). The calculated Fermi contact interaction is, of course, strongly dependent upon the distance between the axial ligand(s) and the metal atom. For the geometries where at least one Pt–O distance is rather short ($[Pt(NH_3)_4(OH)_2]^+$ and $\{[Pt(NH_3)_4(OH)](OH)\}^+$), this Fermi term is always found positive and lying in a range compatible with the experimental value of *K*. As shown in Table II, the calculated Fermi interaction is directly related to the Pt 6s contribution to the SOMO reduced by the internal core polarization. For the tetracoordinated complex, $[Pt(NH_3)_4]^{3+}$, this polarization is the only contribution to the Fermi term and such a structure would imply a negative Fermi value ($A_F = -129$ MHz). It is clear, therefore, from these magnetic observables that the tetracoordinated planar structure of the precursor is not retained for the trapped Pt(III) species. A first hypothesis consists of assuming that a direct ionization of $[Pt(en)_2]^{2+}$ is followed by an approach of the squarates and leads to $[Pt(en)_2(HSq)_2]^+$. In the crystal, however, these axial ligands are located rather far from the platinum atom (3.3 Å) and, owing to the presence of hydrogen bonds, can hardly move toward the metal. Moreover, the $g_\parallel$ direction, which is expected,

(27) Amano, C.; Fujiwara, S. *Bull. Chem. Soc. Jpn.* **1977**, *50*, 1437.
(28) Maki, A. H.; Edelstein, N.; Davidson, A.; Holm, R. H. *J. Am. Chem. Soc.* **1964**, *86*, 4580.
(29) McGarvey, B. R. *Can. J. Chem.* **1975**, *53*, 2498.
(30) Morton, J. R.; Preston, K. F. *J. Magn. Reson.* **1978**, *30*, 577.
(31) Most of the Pt(III) EPR spectra reported in the literature[12,32] have been analyzed by using expressions of the g and hyperfine tensors which contain the normalization coefficient (*N*) of the zero-order ground state and the spin density in the Pt d_{z^2} orbital λ_2. By substituting our experimental g and ^{195}Pt *T* eigenvalues into these equations and by using $P_0 = 1474$ MHz,[30] we found $c_1 = 0.035$, $N = 0.987$, $\lambda_2 = 0.91$, and $K = +472$ MHz.
(32) Barton, J. K.; Szalda, D. J.; Rabinowitz, H. N.; Waszeczak, J. V.; Lippart, S. J. *J. Am. Chem. Soc.* **1979**, *101*, 1434. Uemura, T.; Tomihiro, T.; Hayamizu, K.; Okuno, Y. *Chem. Phys. Lett.* **1987**, *142*, 423. Mehran, F.; Scott, B. A. *Phys. Rev. Lett.* **1973**, *31*, 99.

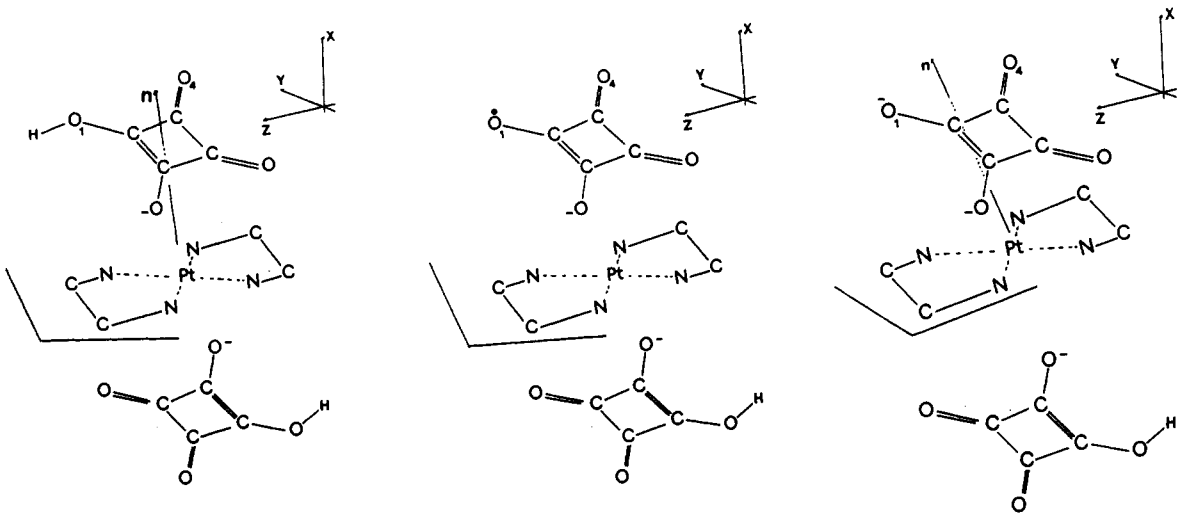

Figure 5. Mechanism of oxidation of $[Pt(en)_2]^{2+}$ in an X-irradiated crystal of $[Pt(en)_2](HSq)_2$. *n* is aligned along the normal to the plane containing the four nitrogen atoms. *XYZ* is the EPR reference frame (the angle between OX and the normal to the PtN_4 plane of the precursor is equal to 4.5°; the angle between OZ and the bisector of the NPtN angle of a ligand is equal to 3°).

in this model, to be perpendicular to the crystallographic PtN_4 plane, makes an angle of 23° with the normal to this plane and clearly indicates that the $Pt(en)_2$ moiety reorientates during the oxidation process. In fact, this $g_\parallel$ direction, which probably points toward the axial ligand(s), is practically oriented along the bisector of the (PtO1,PtO4) angle and makes an angle of 18° only with the Pt–O1 direction. This property is notable because O1 and O4 are more distant from the platinum atom than O2 and O3 (Figure 4b), and yet, the angle between $g_\parallel$ and Pt–O2 or Pt–O3 is more than 50°. These observations show that, probably, O1 plays a special role in the oxidation process and suggest the mechanism shown in Figure 5: under irradiation, the homolytic scission of the OH bond of a hydrogen squarate ion yields a radical centered on O1; this RO type radical can oxidize the neighbor platinum ion and gives rise, formally, to the $C_4O_4^{2-}$ anion. In this process, the four oxygen atoms of the squarate dianion are not equivalent and the unpaired electron is assumed to be mainly delocalized on the O1 and O4 atoms; when the $Pt(en)_2$ moiety moves slightly toward this part of the squarate ion, the PtN_4 plane reorients in order to position the O1C1C4O4 moiety in the axial region. Although this reorientation is rather complex and is probably, in part, governed by the crystal packing, it is in good accordance with the fact that $g_\parallel$, which indicates the normal to the final orientation of the PtN_4 plane, is roughly oriented toward the oxygen of the hydroxyl group. Together with the Xα results, this implies the presence of an axial ligand close to the metal atom. This oxidation of a metal by a radiolytic radical formed by homolytic scission of an OH bond is quite consistent with previous observations of Waltz et al.[33] who showed, by pulsed radiolysis, that in aqueous media the OH radicals can oxidize bis(ethylenediamine)platinum(II) perchlorate. Moreover, the formal formation of $C_4O_4^{2-}$ is not surprising, since the electron capture by a carbon oxyanion has recently been invoked to explain the formation of radical pairs in irradiated croconate crystals.[34] Furthermore, the oxidative behavior of squaric acid toward platinum complexes has already been mentioned, and it was shown previously[35] that the reaction of squaric acid with the tetranuclear platinum(II) complex $[Pt(NH_3)_2C_4O_4]_4$ leads to a blue dinuclear compound with the platinum atom in a formal oxidation state of 2.5.

Acknowledgment. We thank the Swiss National Science Foundation for financial support.

Supplementary Material Available: A list of atomic coordinates of the Pt(II) compound expressed in the Cartesian EPR reference frame *XYZ* (1 page). Ordering information is given on any current masthead page.

(33) Waltz, W. L.; Lilie, J.; Walters, R. T.; Woods, R. J. *Inorg. Chem.* **1980**, *19*, 3284.
(34) Geoffroy, M.; Wermeille, M.; Castan, P.; Deguenon, D.; Bernardinelli, G. *Radat. Phys. Chem.* **1991**, *37*, 279.
(35) Soules, R.; Mosset, A.; Laurent, J. P.; Castan, P.; Bernardinelli, G.; Dalaman, M. *Inorg. Chim. Acta* **1989**, *155*, 105.